Research Square

Preprints are preliminary reports that have not undergone peer review.
They should not be considered conclusive, used to inform clinical practice,
or referenced by the media as validated information.

Effect of TEMPO oxidation and Homogenization Passes on the Properties of Nanocellulose and its Composites

Krishnakant Bhole

krishnakant.bhole@gmail.com

Indian Institute of Science Bangalor

N D Shivakumar

Indian Institute of Science Bangalor

Shakti Singh Chauhan

Institute of Wood Science and Technology

Research Article

Keywords: NFC, Homogenization passes, XRD, Rheology, Bamboo bio-composite

Posted Date: June 26th, 2026

DOI: https://doi.org/10.21203/rs.3.rs-10067346/v1

License: This work is licensed under a Creative Commons Attribution 4.0 International License.
Read Full License

Additional Declarations: No competing interests reported.

Effect of TEMPO oxidation and Homogenization Passes on the Properties of Nanocellulose and its Composites

Abstract

Conventional particleboards and wood-based composites rely on synthetic polymeric adhesives, such as formaldehyde-based resins, which are effective but carcinogenic and environmentally harmful. In this study, bamboo nanofibrillated cellulose (NFC) suspensions prepared via TEMPO oxidation and high-pressure homogenization were explored as natural binders for sustainable composites. Bamboo pulp served as the NFC source, while bamboo particles were used as the reinforcement phase. The effects of homogenization passes (1st and 3rd) were systematically compared. NFC films were characterized by X-ray diffraction (XRD) to determine crystallinity index (CI) and crystallite size (CS), and rheological studies assessed viscosity, storage modulus (G′), and loss modulus (G″). Bio-composites were fabricated by oven-drying (OD) and hot-pressing (HP) the bamboo particle–NFC mixtures, and their mechanical properties were evaluated in terms of modulus of elasticity (MOE), modulus of rupture (MOR), and specific strength. Results showed that increasing homogenization passes reduced CI and CS but enhanced fibrillation and dispersion, leading to improved composite performance under hot pressing. Although the mechanical strength was lower than conventional resin-bonded boards and moisture sensitivity remained a limitation, this study demonstrates the proof-of-concept potential of bamboo NFC as a sustainable binder, offering insights into structure–property–processing relationships and directions for future improvements.

Keywords: NFC, Homogenization passes, XRD, Rheology, Bamboo bio-composite.

1. Introduction:

Nanocellulose (NC) as reinforcement in composites is state of the art. NFC-reinforced bio-composites are gaining significant importance because they are prepared from natural extracts that are abundantly available and environmentally friendly [1, 4]. Bamboo, often referred to as *green gold*, is one of the most versatile natural materials owing to its fast growth rate, renewability, and high strength [5, 6]. NC extracted from bamboo has potential applications in packaging, structural boards, medical products, electronic devices, coatings, automotive, and aeronautic industries [1, 6 - 15]. Bamboo particle-based bio-composites represent a promising pathway for developing green, sustainable, and degradable materials [6, 16, 21].

The demand for biodegradable composites began as early as 1953 [15, 22]. In 1983, Herrick and Turbak developed methods for extracting microfibrillated cellulose (MFC) from wood using high-pressure homogenization [1, 7, 23]. However, converting MFCs to nanoscale remained a challenge. In 2006, Saito introduced TEMPO (2,2,6,6-tetramethylpiperidine-1-oxyl) oxidation, an effective pre-treatment for isolating and fibrillating cellulose fibers [21, 24, 25]. Chemical (TEMPO) and mechanical (homogenization) processes disintegrate fibers into uniform nanoscale fibrils fibers [2, 26 – 28], while centrifugation and ultrasonication ensure homogeneity of NC suspensions [15, 29]. Nanocellulose has since been extracted from various sources such as wood, agricultural residues, bamboo, banana, jute, sisal, eucalyptus, and coir [10, 30, 31], using pre-treatments such as acid hydrolysis, TEMPO oxidation, grinding, ball-milling, enzymatic/bacterial treatments, steam explosion, high-pressure homogenization, centrifugation, and ultrasonication. Acid hydrolysis, typically

with sulfuric or hydrochloric acid, selectively hydrolyzes amorphous cellulose regions while leaving crystalline domains intact, producing nanocrystalline cellulose. However, this often reduces thermal stability due to sulfate group introduction. [1, 30, 32].

Earlier studies investigated NFC suspensions and films using rheology, X-ray diffraction (XRD), Fourier-transform infrared spectroscopy (FTIR), scanning electron microscopy (SEM), transmission electron microscopy (TEM), and atomic force microscopy (AFM), to evaluate viscosity, modulus, crystallinity, and morphology [9, 32, 33]. Numerous researchers have also reported that composites reinforced with NFC showed improved density, porosity, and overall physical and mechanical properties [8, 10, 16, 31, 34].

However, there is limited literature focusing specifically on bamboo-derived NFC, particularly with systematic comparisons of homogenization passes. Bamboo pulp presents unique challenges due to its high silica content, heterogeneous fibrillation behavior, and strong moisture affinity, which affect both NFC preparation and composite performance. Moreover, the influence of homogenization passes on bamboo NFC's crystallinity, rheological behavior, and resulting composite properties has not been adequately addressed. This creates a gap in understanding the processing–structure–property relationships that are critical for advancing NFC-based adhesives.

In this study, we specifically address the research gap related to homogenization passes in bamboo-derived NFC. The work aims to examine how varying the number of homogenization passes influences the crystallinity, rheological behavior, and morphology of NFC extracted from bamboo pulp. By establishing these structure–property relationships, we further investigate how such variations affect the bonding efficiency and mechanical performance of bamboo particle composites prepared by oven drying and hot pressing. Finally, this study also seeks to identify the limitations of bamboo NFC composites, particularly their mechanical strength and moisture sensitivity, and to propose strategies that could enhance their application potential compared to conventional resin-bonded boards.

2. Experimental procedure, materials, and equipment

2.1 Materials

Commercially available bamboo pulp supplied by Harihar Polyfibers, Harihar, Karnataka, India, was used as the source of nanocellulose (NC). The bamboo pulp was stored in a desiccator under dry and sealed conditions at room temperature (25 ± 2 °C) prior to use. Bamboo particles used for composite preparation were prepared in-house, by grinding mature bamboo culms, sieving to a particle size range of –30 + 60 BSS mesh (corresponding to an average size of ~150 μm), and oven-drying at 80 °C to a moisture content of ~8–10%.

TEMPO (2,2,6,6-tetramethylpiperidine-1-oxyl) free radicals and all laboratory-grade reagents, including sodium hypochlorite (NaClO), sodium bromide (NaBr), sodium hydroxide (NaOH), and acetone, were procured from Vasa Scientific Company, Bangalore, and used without further purification. Distilled water was used to prepare all NC suspensions. For rheological characterization, NFC suspensions were prepared at a concentration of 1 wt%.

2.2 Preparation of NFC

2.2.1 TEMPO Oxidation

Nanocellulose preparation was carried out in a two-stage chemo-mechanical process. First, cellulose fibers from bamboo pulp were pretreated and partially defibrillated using the TEMPO oxidation method. In the second stage,

the oxidized cellulose suspension was passed through high-pressure homogenization to generate NFC. Both steps are schematically represented in Figure 1.

The TEMPO process was initiated with 180 gm of never-dried bamboo pulp containing 30% solid content, which was repeatedly washed with distilled water to remove impurities. The washed pulp was dispersed in distilled water and homogenized at 21,000 rpm for 5–15 min to achieve uniform dispersion. The reaction mixture contained TEMPO, sodium bromide (NaBr), and sodium hypochlorite (NaClO) as the oxidizing system. The specific quantities of the constituents are given in Table 1.

Table 1: Cellulose Processing by TEMPO Oxidation

Constituent	Quantity	Action
Bamboo pulp	180 gm	NC Source
2,2,6,6, -Tetramethyl-1-piperidinyloxy (TEMPO)	0.375 gm	Catalyst
Sodium bromide	3.75 gm	Co-Catalyst
Sodium hypochlorite	420 ml	Oxidizing agent
Sodium hydroxide	5/250 gm/ml	Maintain pH
Operating conditions		
pH	10 - 11	
Duration	About 2 hrs.	
Temperature	ambient (25 ± 2 °C)	

During oxidation, NaClO acted as the primary oxidant, while NaBr regenerated the TEMPO catalyst. The pH was continuously monitored and maintained at 10–11 by dropwise addition of NaOH solution. The endpoint of the reaction was determined when no further consumption of NaClO was observed and the pH remained stable, indicating complete oxidation of the hydroxyl groups.

At the end of the reaction, the suspension was washed thoroughly by centrifugation to remove unreacted chemicals. The sediment was repeatedly re-dispersed in distilled water until neutral pH was reached, yielding a stable TEMPO-oxidized pulp suspension for subsequent homogenization.

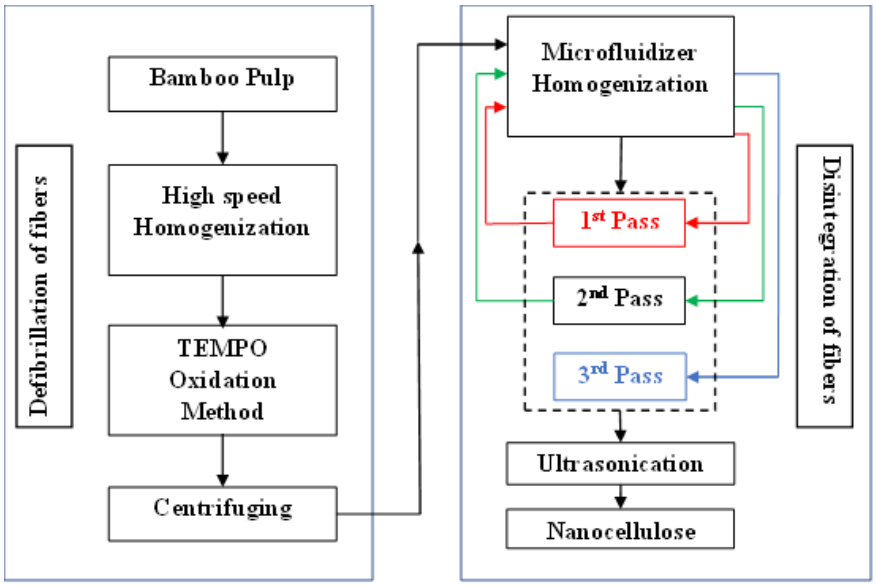


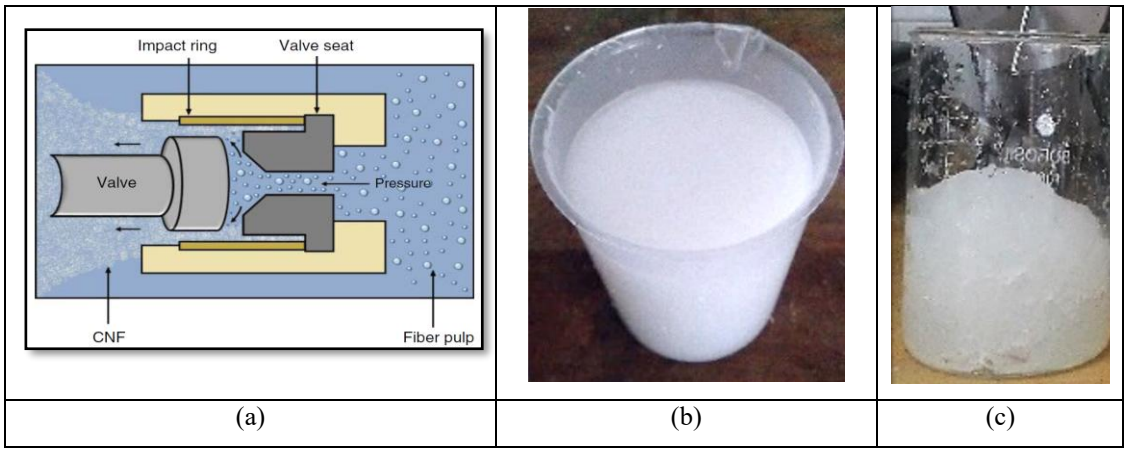
Figure 1: Schematic representation of nanocellulose synthesis via chemo-mechanical process

2.2.2 *Homogenization*

The TEMPO-pretreated cellulose suspension was further fibrillated using a high-pressure homogenizer (M-110P Microfluidizer). The suspension was pressurized up to 30,000 psi and forced through a fixed-geometry interaction chamber with a Z-shaped microchannel of 90 µm. The chamber design ensured constant pressure and reproducibility of the process. Since the intense shear forces generated internal heating, the chamber was cooled by circulating chilled water.

During homogenization, the cellulose fibrils were subjected to high shear and impact stresses that disrupted them into nanoscale dimensions. Additionally, the sudden depressurization at the outlet, from ~30,000 psi to atmospheric conditions, promoted further fibrillation via shear and cavitation effects. The first passage through the chamber produced the 1st pass suspension, while repeated processing under identical conditions generated the 3rd pass suspension. Throughout this study, the 1st pass data are represented in red and the 3rd pass data in blue.

As illustrated in Figure 2 (a – c), the process involves: (a) fibril disintegration in the fixed-geometry chamber [35, 36], (b) uniform NFC suspension with fibril diameters typically ranging from 10–50 nm, and (c) additional fibrillation promoted by outlet depressurization.



(a) (b) (c)

Figure 2: High-pressure homogenization (a) Disintegration of cellulose to NFC [36] *(b) NFC suspension after homogenization (c) Outlet depressurization from ~30,000 psi to ambient, enhancing fibrillation through shear and cavitation.*

2.2.3 *Ultrasonication*

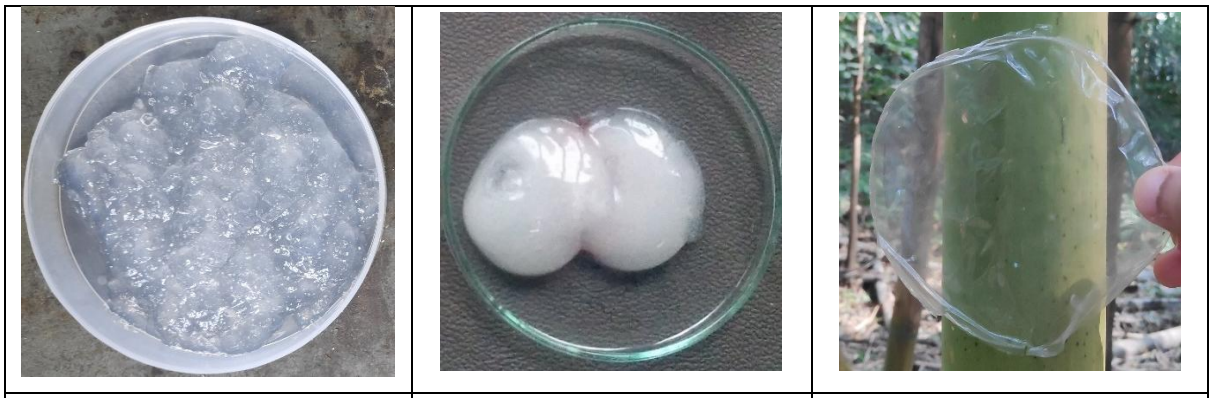
To prevent agglomeration and enhance dispersion stability, both 1st pass and 3rd pass NFC suspensions were subjected to high-intensity ultrasonication. A Hielscher ultrasonic processor (400 W, 24 kHz) was used for ~30 min in a water-jacketed cell with continuous cold-water circulation to control temperature rise. Ultrasonication complemented the microfluidization process by de-bundling residual aggregates and distributing fibrils uniformly in suspension, thereby improving homogeneity and rheological stability.

2.3 NC Sample Preparation for characterization

The synthesized nanocellulose (NC) was characterized in both suspension and film form, and its composites were prepared for mechanical testing. NC films were analyzed using XRD, NC suspensions were studied using rheology, and composites were evaluated by tensile and flexural tests.

As shown in Figure 3 (a–c), the suspension obtained after the 1st pass was partially fibrillated Fig. 3 (a), while the suspension became progressively more homogeneous with additional passes. A fully homogeneous NFC

suspension was obtained after the 3rd pass Fig. (3b). These suspensions were further cast into thin films for XRD characterization Fig. 3 (c).



(a) (b) (c)

Figure 3: Homogenisation passes NC samples (a) NC after 1st pass (b) NC after 3rd pass (c) NC film

2.3.1 X-ray diffraction of NC

NC suspensions were cast into films by drying and then analyzed using X-ray diffraction (XRD). XRD data were collected using a Rigaku SmartLab diffractometer with a Cu Kα source operated at 40 kV and 30 mA. The X-ray beam had a wavelength of 1.54 Å, and scans were performed over a 2θ range of 5°–70°.

2.3.2 Rheological characterization

The viscoelastic behavior of NC suspensions (1 wt%) was studied using an Anton Paar MCR 302 stress-controlled rheometer equipped with a 25 mm parallel plate geometry. Oscillatory shear experiments were performed at a strain amplitude of 5% within the linear viscoelastic region.

2.3.3 Composites preparation for Mechanical tests (tensile and flexural)

Composites were prepared using the 1st pass and 3rd pass NFC suspensions mixed with bamboo powder in a 1:1 weight ratio. The mixture was prepared manually Fig. 4 (a) and transferred into customized tensile and flexural specimen molds Fig. 4 (b) and 4 (c), fabricated according to ASTM standards [34].

Two types of composite samples were fabricated:

1. **Oven-dried (OD)** composites, prepared by drying at 80 °C.
2. **Hot-pressed (HP)** composites, prepared by pressing at 120 °C under 5 MPa for 15 min.

In oven-dried composites, no external pressure was applied. Instead, the hydrogen-bonded CNF network provided the bonding mechanism to hold bamboo particles together, differentiating them from conventional pressurized composites. Mechanical properties were tested using a micro universal testing machine (UTM) with a load capacity of 25 N–10 kN and a crosshead speed of 1 mm/min. Tensile tests were conducted following ASTM D638, and flexural tests were carried out according to ASTM D790.

Sample dimensions were:

- **Tensile tests:** 50 × 12 × 5 mm (OD) and 50 × 12 × 2 mm (HP).
- **Flexural tests:** 35 × 12 × 5 mm (OD) and 35 × 12 × 2 mm (HP).

Each test was performed on five replicates for each condition: OD 1st pass, OD 3rd pass, HP 1st pass, and HP 3rd pass.



(a) (b) (c)

Figure 4: Composite preparation: (a) Mixing NFC suspension with bamboo powder, (b) tensile test specimens, (c) flexural test specimens

3. Results and Discussion:

The formation of NFC from bamboo pulp after TEMPO oxidation and homogenization was earlier confirmed by SEM morphological analysis [34]. The present work focuses on comparing the structural changes in NFC obtained after the 1st and 3rd homogenization passes.

3.1 XRD

The bamboo NFC suspension was characterized using XRD, showing the presence of a typical cellulose I structure [33]. The diffractogram (Fig. 5) displays reflections at 2θ ≈ 14.5°, 16.5°, 22.5° (200 plane), and 34.5°, consistent with cellulose I reported in the literature. The prominent peak at 22.5° corresponds to the 200 crystallographic plane obtained after TEMPO pre-treatment and microfluidization. Both the crystallite size (CS) and crystallinity index (CI) were calculated using standard methods: the Segal peak-height method [22] for CI and the Scherrer equation for CS. The CI is expressed as:

$$\mathrm{CI} = \frac{I_{002} - I_{am}}{I_{002}}$$

where I_{002} is the maximum intensity of the 002 lattice plane, and I_{am} is the diffraction intensity at 2θ=18°. The average CS is obtained from the Debye Scherrer Equation as,

$$\mathrm{CS} = \frac{k\lambda}{\beta \cos\theta}$$

Where k is the Scherrer constant (0.9), λ is the X-ray wavelength (1.548 A°), β is the full width at half maximum peak (FWHM)in radians, and θ is the angle of diffraction.

The CI decreased slightly from 59% (1st pass) to 55% (3rd pass), while the CS reduced by ~7.3% (Table 2). This reduction can be attributed to the repeated action of high-pressure homogenization (MFD), which subjects fibrils to shear, cavitation, and impact stresses that disrupt crystalline domains and create new amorphous regions. Similar decreases in CI during mechanical fibrillation of cellulose have been reported in earlier studies [26].

At the same time, the TEMPO oxidation step plays a stabilizing role. By selectively oxidizing the hydroxyl groups, TEMPO pre-treatment weakens lignin/hemicellulose interactions and promotes fibril separation, partially

counteracting crystallinity loss during homogenization [6, 11, 14, 20, 37]. This explains why the observed CI reduction is moderate, even after multiple homogenization passes and ultrasonication.

During ultrasonication (US, 24 kHz, 400 W), cavitation generates microbubbles that collapse rapidly, producing transient high shear and localized hotspots. Although extreme localized temperatures are sometimes reported in cavitation literature, in this study the water-cooled system maintained bulk temperature stability, limiting thermal degradation of cellulose. The dominant effect of US is therefore mechanical de-agglomeration rather than bulk thermal changes.

It is noteworthy that surface charge (zeta potential) and fibril particle-size distribution, which strongly influence crystallinity retention and dispersion stability, were not measured in the present work. Their absence is acknowledged as a limitation, and these properties will be prioritized in follow-up studies for better understanding of structure–property relationships.

Overall, the XRD analysis shows that while increasing homogenization passes decreases CI and CS modestly, the generation of smaller, more fibrillated NFCs enhances surface area and hydrogen-bonding potential. These structural changes are expected to influence the rheology and interfacial bonding in bamboo particle composites, as discussed in subsequent sections.

Table 2: NFC properties calculated from XRD results

	Crystallinity Size (nm)	**Crystallinity Index (%)**	**MFD Time (Hr)**
1st Pass	1.4475	59	2
3rd Pass	1.3429	55	6

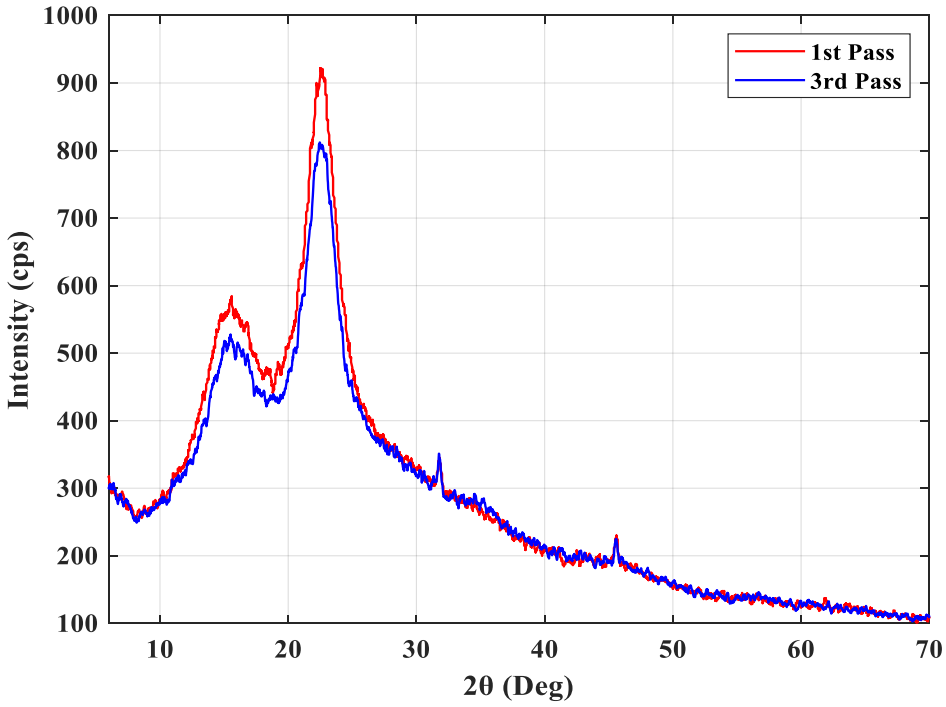


Figure 5: XRD patterns of NFC films after 1st and 3rd homogenization passes showing cellulose I peaks

3.2 Rheology

Figure 6 shows the viscosity variation as a function of the shear rate for NFC suspensions at 1 wt% concentration, tested in parallel plate configuration. For the present experimental scenario, the prime factors like flocculation [39], shear-thinning [25, 27], preferential orientation [40], fiber aspect ratio, the number of microfluidizers passes [7], and the degree of fiber entanglement [41] govern the thixotropic properties. The viscosity (η) as a function of shear rate (γ) can be fitted with a power-law with an appropriate flow index (k), and exponent (α) is given by,

$$\eta = k\gamma^{-\alpha}$$

In the present study, the value of the exponent ranges from 0.9 to 0.98, which shows the non-Newtonian behavior of bamboo NFC aqueous suspension [28, 42], which is comparable to previously reported work [4, 15]. TEMPO treated NFC yielded long fibers after the first pass through the homogenizer. Further, passing it for the third time decreases the aspect ratio of the fibers, leading to flocculation. Previous studies reported that the intrinsic viscosity is proportional to the square of the aspect ratio [43]. Our findings are consistent with this result, as the average viscosity of first-pass NFC is higher than the third pass, as listed in Table 3. However, it decreases monotonically in both cases. The % change in the viscosity is observed to be approximately 81 %. This substantial reduction is due to the presence of 1 wt % consistency [34] of pure NC and excessive fibrillation and disintegration of fibers after several passes through micro fluidization and ultrasonication processes [44], Here, microfluidization primarily reduced fibril length and aspect ratio, while ultrasonication mainly prevented re-flocculation and improved dispersion uniformity [24, 41].

The experiment was further extended to determine the viscoelastic properties of the NC gel. As reported by [34], the DMA yielded a constant storage modulus and loss modulus for increasing temperature. Similar behavior is reflected in the rheological properties for changing angular frequencies. Figure 7 shows the relationship of storage modulus (G'), and loss modulus (G") as a function of angular frequency for two different passes. A relative increase of nearly 84% and 103% in G' and G" values are observed, respectively. The plateau region of the G' curve indicates no phase transition due to the flexibility [45] and stability of the interconnected fibers. It can be inferred from this result that the entangled nanofibers form a network-like structure [2] responsible for the constant elastic regime. Additionally, shear-thinning due to the unidirectional rotation of the plate increases the storage modulus [18]. In some of the recent studies reported by [18, 34], the NC gel support that G' > G" and tanδ < 1 show no viscous dissipation, the elastic property being predominant. These rheological differences between 1st and 3rd pass suspensions directly influence interfacial bonding and composite performance, as discussed in Section 3.3.

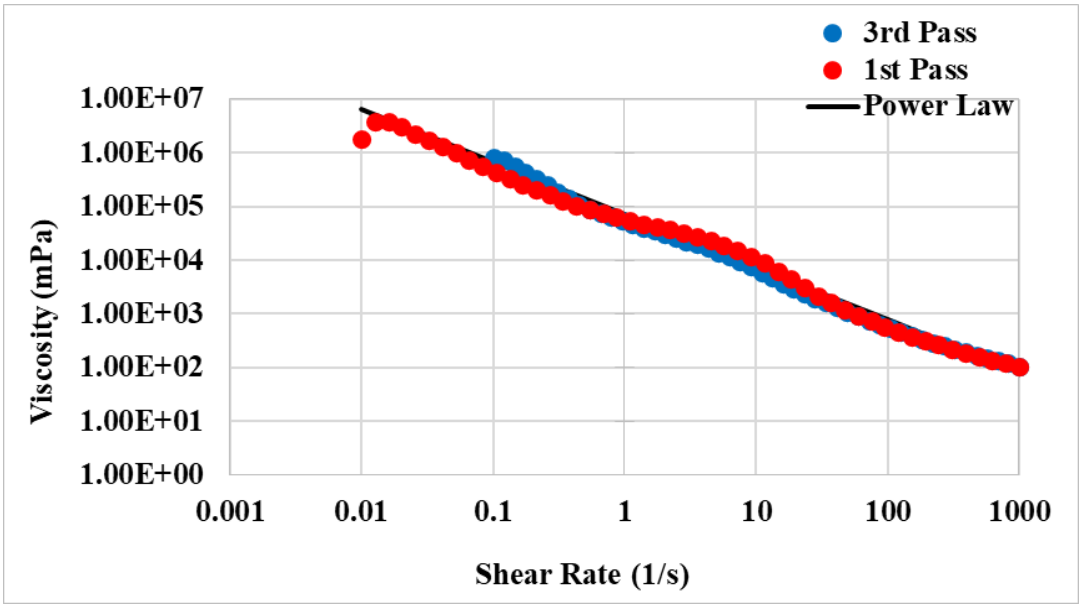


Figure 6: Rheology Viscosity

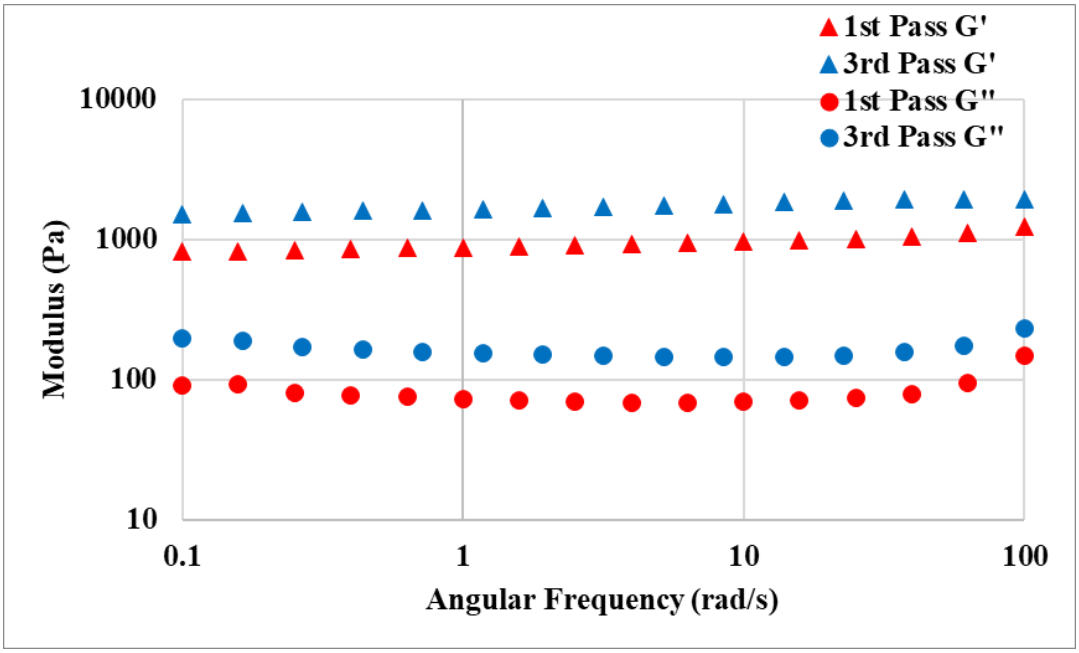


Figure 7: Rheology G' and G"

Table 3: Rheology results

Rheology Sample	Average Viscosity (Pas)	Average G' (Pa)	Average G'' (Pa)
1st Pass	443.3	1583.1	146.3
3rd Pass	82.4	984.4	111.7

3.3 Mechanical Test:

The NC, after mechanical characterization techniques, is used to prepare green composites using bamboo particles. In the previous work by [34], the mechanical properties are analyzed based on the preparation methods and correlated with the binding nature of CNF. However, the present paper emphasizes evaluating mechanical properties (MOE, MOR, and specific strength) depending on the number of homogenization passes and the crystallographic structure of the NFC. Figures 8 and 9 show the stress-strain curves of the tensile test showing the 1st and 3rd pass for OD and HP samples, respectively. From table 4, it can be observed that the MOE value increased by 83% from 1st to the 3rd pass for OD samples and 127% for HP samples. It can be noted that although crystallinity decreased with additional fibrillation, the improved dispersion and surface area of 3rd pass NFC enhanced interfacial bonding, leading to superior composite performance. However, the mechanical properties of the composites prepared from the same NFCs yield different results. Figures 10 and 11 show the stress-strain curves of the flexural test showing the 1st and 3rd pass for OD and HP samples, respectively. The MOR value increased by 1.4 and 1.8 after 3rd pass for OD and HP samples, respectively. Interestingly, specific tensile strength was lower for 1st pass composites, but improved significantly for 3rd pass composites in both OD and HP conditions. This improvement is attributed to finer fibrils creating stronger particle–fibril networks and more efficient load transfer.

Table 4: Tensile and flexural test results comparison

Sample Type		**MOE (MPa)**	**MOR (MPa)**	**Specific Strength (kN/kg)**	
				Tensile	**Flexural**
OD	1st Pass	28.8	0.27	0.8942	1.3107
	3rd Pass	52.8	0.38	0.9834	1.8385
HP	1st Pass	1078	3.3	0.8307	4.1401
	3rd Pass	2448	6.0	1.1533	7.6484

The CI directly influences NFC fibers' tensile strength and MOR due to their compact composition resulting from the cross-linked molecular structure [20]. Additionally, the CI governs G values, which determine the composite reinforcement [13, 46]. The mixing of NFC aqueous suspension with the bamboo particles possibly reduces the global CI of the composite because of the addition of amorphous material [17]. However, the synthesis and manufacturing processes like delignification and hot-pressing enhance the mechanical properties of the bamboo [20]. During the synthesis stage, the addition of TEMPO creates many carboxyl groups that induce charged particles on the surface of the bamboo cell walls [7, 34]. After the delignification process, the bamboo structure becomes more porous, making the cell walls susceptible to shearing [12], which aids the fibrillation process of NFC and bonds the bamboo composites effectively after densification. However, mechanical and chemical treatment of NFC lasts nearly 6 hours; the excessive removal of lignin followed by oven drying and hot-pressing processes lead to brittle fracture of the specimens [34]. The results reveal that higher CI NFC does not necessarily yield stronger composites; instead, fibril dispersibility and interfacial adhesion dominate performance. This

explains why 3rd pass NFC, despite having slightly lower CI, produced composites with superior MOE and MOR — a key novelty of this study, consistent with [47]. One limitation of these binder-free bamboo–NFC composites is their sensitivity to moisture, which can compromise stability and strength. Future work will explore hydrophobic surface treatments or hybridization with biodegradable additives to address this limitation.

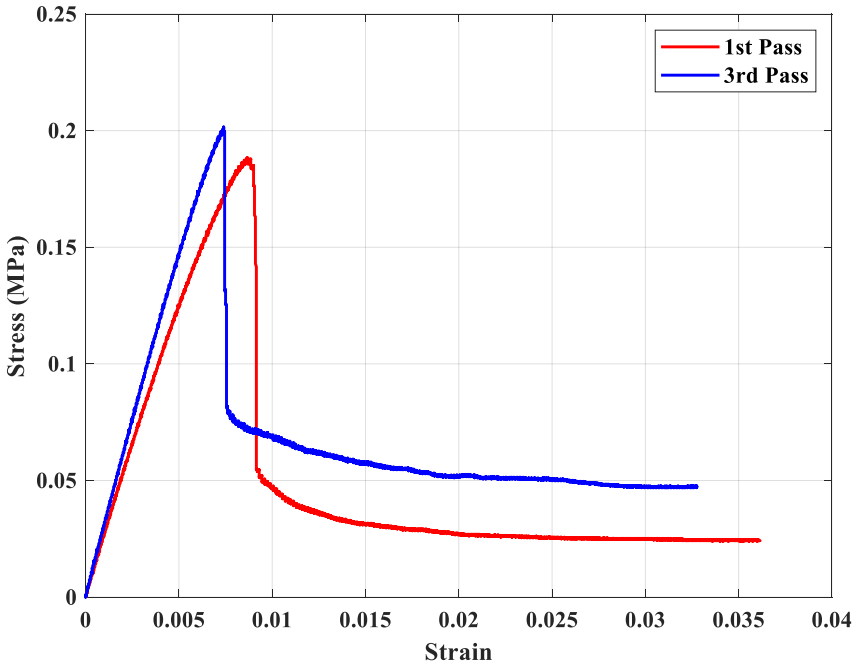


Figure 8: Tensile stress-strain curves for Oven Dried Samples 1st pass and 3rd pass

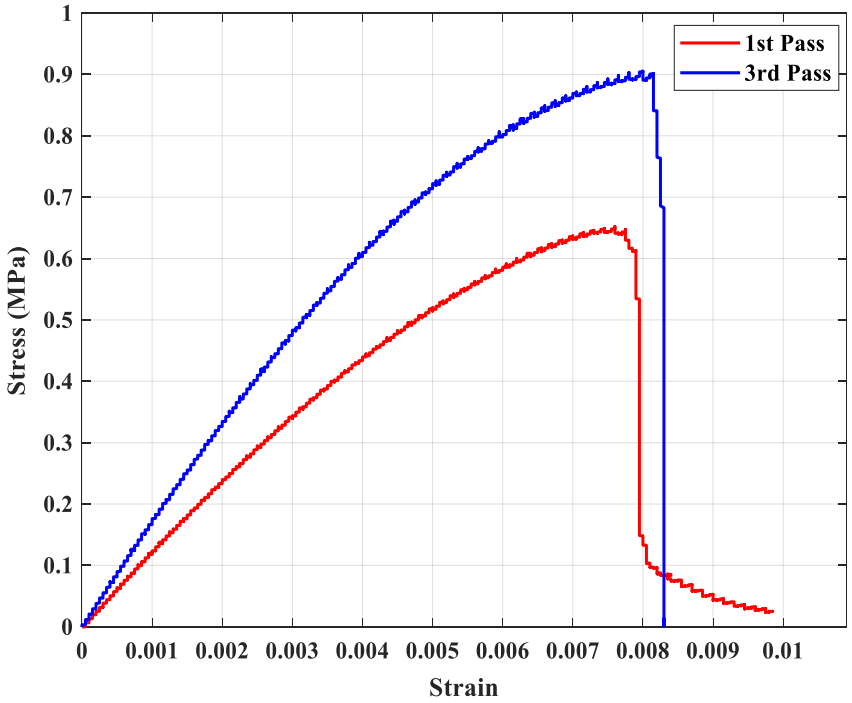


Figure 9: Tensile stress-strain curves for Hot Pressed Samples 1st pass and 3rd pass

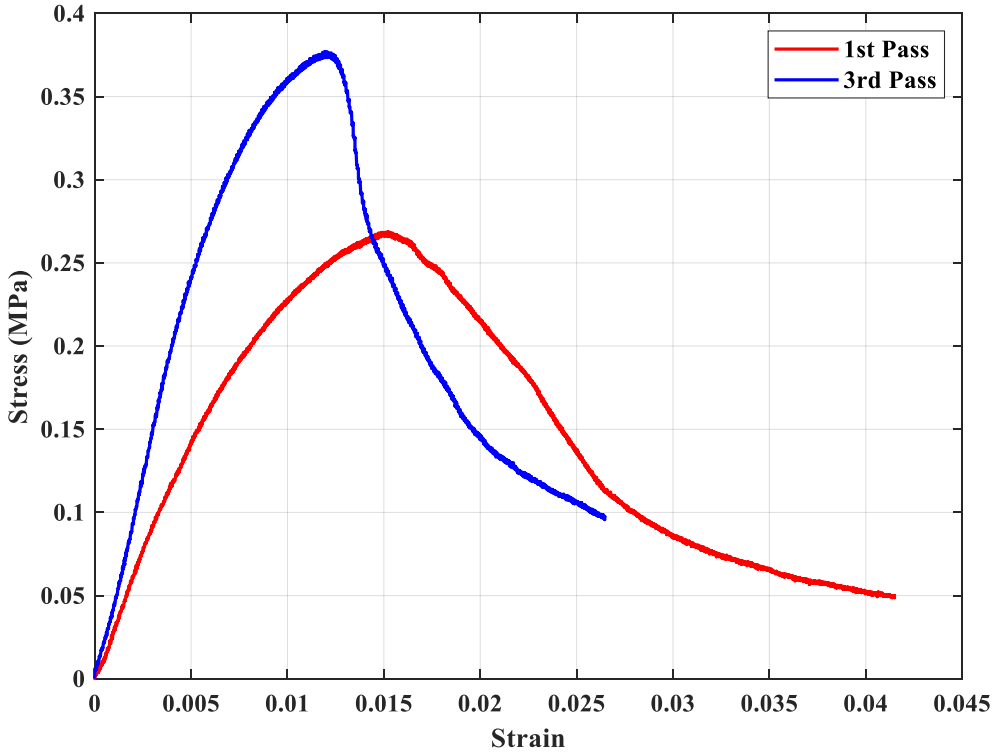


Figure 10: Flexural stress-strain curves for Oven Dried Samples 1st pass and 3rd pass

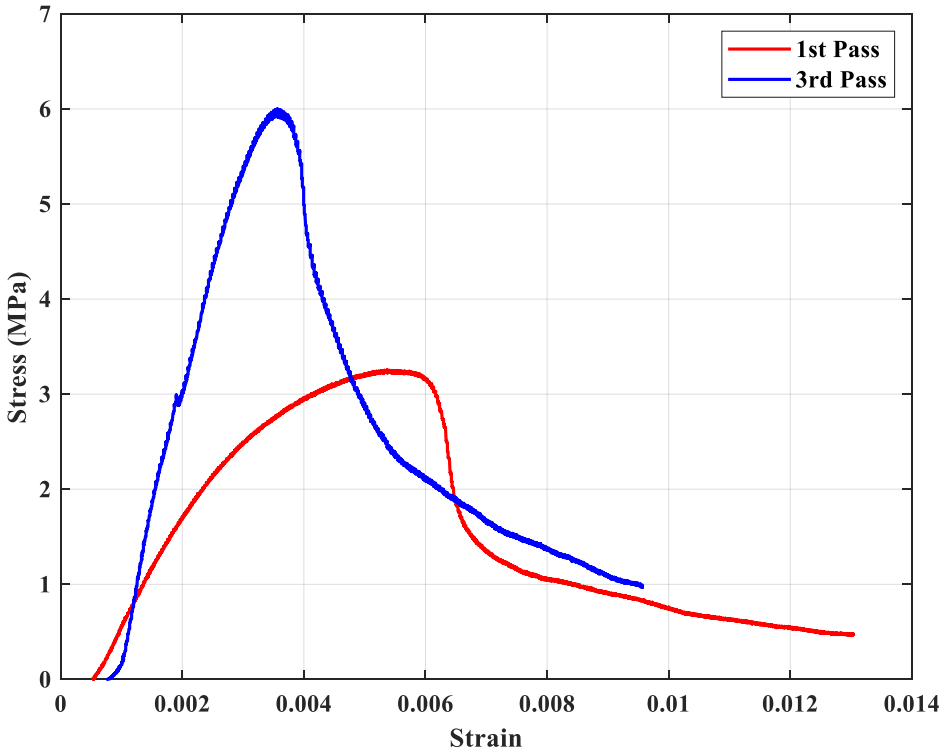


Figure 11: Flexural stress-strain curves for Hot Pressed Samples 1st pass and 3rd pass

4. Summary and conclusions:

The focus of this paper was to investigate NC properties after the 1st and 3rd pass of homogenization and evaluate the mechanical properties of composites prepared out of them. NC was extracted successfully from the bamboo pulp using the TEMPO oxidation and microfluidic homogenization after 1st and 3rd pass. Rheological and crystallographic studies were carried out on NC suspension and its films. From XRD studies, CS is decreased by 7.3 % from 1st to 3rd pass, and CI is also reduced for 3rd pass. Similarly, the viscosity of 3rd pass NC was reduced by ~81% due to disintegration of the NFC network after prolonged homogenization. Both storage modulus (G′) and loss modulus (G″) decreased compared to the 1st pass, but their frequency dependence confirmed stable gel-like behaviour with G′ > G″.

Oven drying and hot press methods effectively held the blend of NFC and bamboo particles to form composites. In tensile and flexural testing of composites, the 3rd pass HP sample showed superior results in MOE, MOR, and specific strength among the other three, viz., 1st pass OD, 1st pass HP, and 3rd pass OD. This demonstrates that composite performance depends more on fibril dispersibility and interfacial bonding than on intrinsic crystallinity, a key novel finding compared to earlier NFC studies. TEMPO oxidation followed by homogenization, centrifuging, and ultrasonication were suitable methods for extracting NFC using bamboo as a source. While crystallinity decreased modestly after homogenization, TEMPO oxidation helped stabilize fibrils and limit crystallinity loss, ensuring adequate structural integrity for composite applications. However, the viscosity reduced drastically from 1st to 3rd pass. These two properties further govern the mechanical properties of the composites. Bamboo NFC improved MOE, MOR, and specific strength of the 3rd pass composites for both the fabrication techniques (OD and HP) in fewer passes compared to literature studies. The findings of this study reveal that repeated microfluidization of bamboo pulp yields a homogenized NFC suspension that binds well with the same reinforcement material (bamboo particles) to prepare composites by enhancing the morphological and mechanical properties. A limitation of this study is that composites were prepared at a fixed 1:1 bamboo:NFC ratio and surface charge/zeta potential was not measured. Future work should explore different ratios, zeta potential analysis, and surface modifications to improve moisture stability. Another limitation is the absence of direct morphological characterization of NFC by AFM or TEM. However, previous studies have reported that TEMPO-prepared NFC typically exhibits fibril widths in the 5–20 nm range [9, 24, 32]. Future work will include AFM/TEM imaging to directly validate fibril dimensions. It can be concluded that NC prepared with bamboo is suitable to prepare sustainable, low-cost, and environmentally friendly bio-composites.

Funding: The authors received no specific funding for this work.

Conflict of interest: The authors declare that they have no conflicts of interest to report regarding the present study.

Declarations

- **Ethical approval**: Not applicable.
- **Consent to participate**: Not applicable.
- **Consent to publish**: All authors consent to the publication of this manuscript.

REFERENCES:

[1] C. Vilela, R. J. B. Pinto, A. R. P. Figueiredo, C. P. Neto, A. J. D. Silvestre, and C. S. R. Freire, "1 Development and applications of cellulose nanofibres based polymer nanocomposites," *Adv. Compos. Mater. Prop. Appl.*, pp. 1–65, 2017, doi: 10.1515/9783110574432-001.

[2] B. Li *et al.*, "Cellulose nanocrystals prepared via formic acid hydrolysis followed by TEMPO-mediated oxidation," *Carbohydr. Polym.*, vol. 133, pp. 605–612, 2015, doi: 10.1016/j.carbpol.2015.07.033.

[3] C. Chen and L. Hu, "Nanoscale Ion Regulation in Wood-Based Structures and Their Device Applications," *Adv. Mater.*, vol. 33, no. 28, pp. 1–28, 2021, doi: 10.1002/adma.202002890.

[4] C. Honorato, V. Kumar, J. Liu, H. Koivula, C. Xu, and M. Toivakka, "Transparent nanocellulose-pigment composite films," *J. Mater. Sci.*, vol. 50, no. 22, pp. 7343–7352, 2015, doi: 10.1007/s10853-015-9291-7.

[5] S. Jansiri, A. Deenu, B. Puangsin, S. Sungkaew, and S. Kamthai, "Characterization of sweet bamboo (Dendrocalamus asper Backer) kraft pulp filled in poly(lactic acid)/polybutylene succinate blend composite," *Polym. Compos.*, vol. 42, no. 10, pp. 5090–5100, 2021, doi: 10.1002/pc.26207.

[6] W. Gu *et al.*, "Study on preparation of lignin-containing nanocellulose from bamboo parenchyma," *J. Renew. Mater.*, vol. 10, no. 2, pp. 385–399, 2022, doi: 10.32604/jrm.2022.016457.

[7] A. Naderi, T. Lindström, J. Erlandsson, J. Sundström, and G. Flodberg, "A comparative study of the properties of three nano-fibrillated cellulose systems that have been produced at about the same energy consumption levels in the mechanical delamination step," *Nord. Pulp Pap. Res. J.*, vol. 31, no. 3, pp. 364–371, 2016, doi: 10.3183/npprj-2016-31-03-p364-371.

[8] M. Pervaiz and M. M. Sain, "Sheet-molded polyolefin natural fiber composites for automotive applications," *Macromol. Mater. Eng.*, vol. 288, no. 7, pp. 553–557, 2003, doi: 10.1002/mame.200350002.

[9] V. Landry, A. Alemdar, and P. Blanchet, "Nanocrystalline cellulose: Morphological, physical, and mechanical properties," *For. Prod. J.*, vol. 61, no. 2, pp. 104–112, 2011, doi: 10.13073/0015-7473-61.2.104.

[10] G. H. D. Tonoli *et al.*, "Cellulose sheets made from micro/nanofibrillated fibers of bamboo, jute and eucalyptus cellulose pulps," *Cellul. Chem. Technol.*, vol. 53, no. 3–4, pp. 291–305, 2019, doi: 10.35812/cellulosechemtechnol.2019.53.29.

[11] Y. Liu and H. Hu, "X-ray diffraction study of bamboo fibers treated with NaOH," *Fibers Polym.*, vol. 9, no. 6, pp. 735–739, 2008, doi: 10.1007/s12221-008-0115-0.

[12] C. Chen *et al.*, "Rapid Processing of Whole Bamboo with Exposed, Aligned Nanofibrils toward a High-Performance Structural Material," *ACS Nano*, vol. 14, no. 5, pp. 5194–5202, 2020, doi: 10.1021/acsnano.9b08747.

[13] W. Chen, H. Yu, and Y. Liu, “Preparation of millimeter-long cellulose i nanofibers with diameters of 30-80 nm from bamboo fibers,” *Carbohydr. Polym.*, vol. 86, no. 2, pp. 453–461, 2011, doi: 10.1016/j.carbpol.2011.04.061.

[14] M. Yu, R. Yang, L. Huang, X. Cao, F. Yang, and D. Liu, “Preparation and characterization of bamboo nanocrystalline cellulose,” *BioResources*, vol. 7, no. 2, pp. 1802–1812, 2012, doi: 10.15376/biores.7.2.1802-1812.

[15] I. Besbes, M. R. Vilar, and S. Boufi, “Nanofibrillated cellulose from Alfa, Eucalyptus and Pine fibres: Preparation, characteristics and reinforcing potential,” *Carbohydr. Polym.*, vol. 86, no. 3, pp. 1198–1206, 2011, doi: 10.1016/j.carbpol.2011.06.015.

[16] N. Saba *et al.*, “Thermal and dynamic mechanical properties of cellulose nanofibers reinforced epoxy composites,” *Int. J. Biol. Macromol.*, vol. 102, pp. 822–828, 2017, doi: 10.1016/j.ijbiomac.2017.04.074.

[17] N. S. Sulaiman, R. Hashim, M. H. M. Amini, O. Sulaiman, and S. Hiziroglu, “Evaluation of the properties of particleboard made using oil palm starch modified with epichlorohydrin,” *BioResources*, vol. 8, no. 1, pp. 283–301, 2013, doi: 10.15376/biores.8.1.283-301.

[18] Y. Zhu *et al.*, “Cellulose gel dispersions: fascinating green particles for the stabilization of oil/water Pickering emulsion,” *Cellulose*, vol. 24, no. 1, pp. 207–217, 2017, doi: 10.1007/s10570-016-1093-9.

[19] K. Dimic-Misic, T. Maloney, and P. Gane, “Effect of fibril length, aspect ratio and surface charge on ultralow shear-induced structuring in micro and nanofibrillated cellulose aqueous suspensions,” *Cellulose*, vol. 25, no. 1, pp. 117–136, 2018, doi: 10.1007/s10570-017-1584-3.

[20] J. Li, C. Chen, J. Y. Zhu, A. J. Ragauskas, and L. Hu, “In Situ Wood Delignification toward Sustainable Applications,” *Accounts Mater. Res.*, vol. 2, no. 8, pp. 606–620, 2021, doi: 10.1021/accountsmr.1c00075.

[21] K. Dimic-Misic, T. Maloney, G. Liu, and P. Gane, “Micro nanofibrillated cellulose (MNFC) gel dewatering induced at ultralow-shear in presence of added colloidally-unstable particles,” *Cellulose*, vol. 24, no. 3, pp. 1463–1481, 2017, doi: 10.1007/s10570-016-1181-x.

[22] L. Segal, J. J. Creely, A. E. Martin, and C. M. Conrad, “An Empirical Method for Estimating the Degree of Crystallinity of Native Cellulose Using the X-Ray Diffractometer,” *Text. Res. J.*, vol. 29, no. 10, pp. 786–794, 1959, doi: 10.1177/004051755902901003.

[23] and K. R. S. ALBIN F. TURBAK, FRED W. SNYDER, “Turback-1983.pdf,” *Microfibrillated cellulose, a new cellulose product: properties, uses, and commercial potential*. pp. 815–827, 1983.

[24] T. Saito, Y. Nishiyama, J. L. Putaux, M. Vignon, and A. Isogai, “Homogeneous suspensions of individualized microfibrils from TEMPO-catalyzed oxidation of native cellulose,” *Biomacromolecules*, vol. 7, no. 6, pp. 1687–1691, 2006, doi: 10.1021/bm060154s.

[25] R. J. Crawford, K. J. Edler, S. Lindhoud, J. L. Scott, and G. Unali, “Formation of shear thinning gels from partially oxidised cellulose nanofibrils,” *Green Chem.*, vol. 14, no. 2, pp. 300–303, 2012, doi:

10.1039/c2gc16302k.

[26] F. K. Andrade *et al.*, “Stable microfluidized bacterial cellulose suspension,” *Cellulose*, vol. 26, no. 10, pp. 5851–5864, 2019, doi: 10.1007/s10570-019-02512-y.

[27] F. Bettaieb, O. Nechyporchuk, R. Khiari, M. F. Mhenni, A. Dufresne, and M. N. Belgacem, “Effect of the oxidation treatment on the production of cellulose nanofiber suspensions from Posidonia oceanica: The rheological aspect,” *Carbohydr. Polym.*, vol. 134, pp. 664–672, 2015, doi: 10.1016/j.carbpol.2015.07.091.

[28] T. Pääkkönen, K. Dimic-Misic, H. Orelma, R. Pönni, T. Vuorinen, and T. Maloney, “Effect of xylan in hardwood pulp on the reaction rate of TEMPO-mediated oxidation and the rheology of the final nanofibrillated cellulose gel,” *Cellulose*, vol. 23, no. 1, pp. 277–293, 2016, doi: 10.1007/s10570-015-0824-7.

[29] S. Ramesh and P. Radhakrishnan, “Cellulose nanoparticles from agro-industrial waste for the development of active packaging,” *Appl. Surf. Sci.*, vol. 484, no. March, pp. 1274–1281, 2019, doi: 10.1016/j.apsusc.2019.04.003.

[30] B. Deepa *et al.*, “Utilization of various lignocellulosic biomass for the production of nanocellulose: a comparative study,” *Cellulose*, vol. 22, no. 2, pp. 1075–1090, 2015, doi: 10.1007/s10570-015-0554-x.

[31] H. Yano and K. Abe, “Reinforcement of Cellulose Nanofibers On the Stiffness and Strength of Composite Sheets Under Dry and Wet Conditions,” 2022.

[32] J. Zeng, F. Hu, Z. Cheng, B. Wang, and K. Chen, “Isolation and rheological characterization of cellulose nanofibrils (CNFs) produced by microfluidic homogenization, ball-milling, grinding and refining,” *Cellulose*, vol. 28, no. 6, pp. 3389–3408, 2021, doi: 10.1007/s10570-021-03702-3.

[33] A. El Oudiani, Y. Chaabouni, S. Msahli, and F. Sakli, “Crystal transition from cellulose i to cellulose II in NaOH treated Agave americana L. fibre,” *Carbohydr. Polym.*, vol. 86, no. 3, pp. 1221–1229, 2011, doi: 10.1016/j.carbpol.2011.06.037.

[34] K. Bhole, N. D. Shivakumar, S. S. Chauhan, and S. Tonannavar, “Cellulose nanofiber networked bamboo particle-based biocomposites,” *Polym. Compos.*, vol. 43, no. 2, pp. 977–986, 2022, doi: 10.1002/pc.26427.

[35] M. S. Kristiina Oksman and Aji P Mathew, Alexander Bismarck, Orlando Rojas, *HANDBOOK OF GREEN MATERIALS ? Bionanomaterials: separation processes, characterization and properties*. 2019.

[36] H. Kargarzadeh, I. Ahmad, and S. Thomas, *Handbook of Cellulose Nanocomposites.* 2017.

[37] K. Daicho, T. Saito, S. Fujisawa, and A. Isogai, “The Crystallinity of Nanocellulose: Dispersion-Induced Disordering of the Grain Boundary in Biologically Structured Cellulose,” *ACS Appl. Nano Mater.*, vol. 1, no. 10, pp. 5774–5785, 2018, doi: 10.1021/acsanm.8b01438.

[38] B. Fan *et al.*, “Natural cellulose nanofiber extracted from cell wall of bamboo leaf and its derived

multifunctional aerogel," *Polym. Compos.*, vol. 39, no. 11, pp. 3869–3876, 2018, doi: 10.1002/pc.24419.

[39] T. Salo, K. Dimic-Misic, P. Gane, and J. Paltakari, "Application of pigmented coating colours containing MFC/NFC: Coating properties and link to rheology," *Nord. Pulp Pap. Res. J.*, vol. 30, no. 1, pp. 165–178, 2015, doi: 10.3183/npprj-2015-30-01-p165-178.

[40] K. M. O. Hakansson, F. Lundell, L. Prahl-Wittberg, and L. D. Söderberg, "Nanofibril Alignment in Flow Focusing: Measurements and Calculations," *J. Phys. Chem. B*, vol. 120, no. 27, pp. 6674–6686, 2016, doi: 10.1021/acs.jpcb.6b02972.

[41] A. Naderi, T. Lindström, and T. Pettersson, "The state of carboxymethylated nanofibrils after homogenization-aided dilution from concentrated suspensions: A rheological perspective," *Cellulose*, vol. 21, no. 4, pp. 2357–2368, 2014, doi: 10.1007/s10570-014-0329-9.

[42] Y. F. Zhang, P. R. Zhang, J. Wu, Q. X. Jia, and X. Y. Liu, "The rheological properties of bamboo cellulose pulp/ionic liquid system," *IOP Conf. Ser. Mater. Sci. Eng.*, vol. 137, no. 1, 2016, doi: 10.1088/1757-899X/137/1/012071.

[43] A. M. Wierenga and A. P. Philipse, "Low-shear viscosity of isotropic dispersions of (Brownian) rods and fibres; a review of theory and experiments," *Colloids Surfaces A Physicochem. Eng. Asp.*, vol. 137, no. 1–3, pp. 355–372, 1998, doi: 10.1016/S0927-7757(97)00262-8.

[44] A. Naderi, T. Lindström, and J. Sundström, "Repeated homogenization, a route for decreasing the energy consumption in the manufacturing process of carboxymethylated nanofibrillated cellulose?," *Cellulose*, vol. 22, no. 2, pp. 1147–1157, 2015, doi: 10.1007/s10570-015-0576-4.

[45] G. A. Van Aken, L. Oliver, and E. Scholten, "Rheological effect of particle clustering in gelled dispersions," *Food Hydrocoll.*, vol. 48, pp. 102–109, 2015, doi: 10.1016/j.foodhyd.2015.02.001.

[46] I. Sakurada, Y. Nukushina, and T. Ito, "Experimental determination of the elastic modulus of crystalline regions in oriented polymers," *J. Polym. Sci.*, vol. 57, no. 165, pp. 651–660, 1962, doi: 10.1002/pol.1962.1205716551.

[47] N. S. Sulaiman, R. Hashim, S. Hiziroglu, M. H. M. Amini, O. Sulaiman, and M. Ezwanselamat, "Rubberwood particleboard manufactured using epichlorohydrin-modified rice starch as a binder," *Cellul. Chem. Technol.*, vol. 50, no. 2, pp. 329–338, 2016.